PERFORMANCE COMPARISON BETWEEN TWO DIFFERENT INJECTOR CONFIGURATIONS IN A HYBRID ROCKET

C. Carmicino, A. Russo Sorge
Department of Space Science and Engineering "L.G. Napolitano",
University of Naples "Federico II", Napoli, Italy

The hybrid rocket engine provides several well-defined advantages over both solid-propellant and liquid-propellant motors. Thrust tailoring and stop-restart capability, its safety, simplicity and lower cost, the latter deriving also from reduced manufacturing tolerances, are among the hybrid's most attractive features which often make hybrid motor the rocket chosen by both universities and amateur rocket enthusiasts.

The solid fuel regression rate is the fundamental parameter needed for modelling the hybrid internal ballistic but, although hybrids are known since 1930, a thorough knowledge of the regression process is still somewhat lacking. For the sake of simplicity, it is often assumed that, in the classical hybrids, the regression rate is only mass flux dependent according to the semi-empirical relationship $\dot{r} \propto G_{ox}^{n}$, with n variable between 0.6 and 0.8. Actually this assumption can lead to significant disagreements between the expected and the measured regression rates.

One reason is certainly represented by the influence of the oxidiser injection characteristics upon the combustor inlet conditions. Indeed, changing the injector configuration, the general motor behaviour will be influenced.

In this paper, a comparison between the experimental results achieved with two distinct injector set-ups is addressed. Average fuel consumption and local regression rate measurements, the latter performed with the ultrasound pulse-echo technique, were used for this purpose. A conical subsonic nozzle and a radial injector were selected to generate different conditions for the oxidiser at the entrance of the fuel port. The axial injector, in particular, is considered interesting because of its easy design and the remarkable feature that, as demonstrated also in Ref. [1], it produces a stable combustion with no substantial pressure oscillations due to the large hot gas recirculation zone inside the combustion port. In order to take advantage of this aspect, it is necessary to investigate the regression rate behaviour under the flow field generated by this injector and, then, most of the tests were carried out on this configuration.

Experimental apparatus and procedure for experimental investigations

A scheme of the test facility is given in Ref. [2]. Gaseous oxygen is supplied at mass flow rates up to 0.3 *kg/s* that are measured with a venturi tube. The oxygen is injected into the chamber through a converging nozzle whose exit diameter is 8 *mm*. The exit Mach number is at most 0.39. Nitrogen is purged into the chamber by a switch valve (oxygen or nitrogen) for the burn out and in case of accident. The ignition was accomplished using a pyrotechnic igniter.

The axisymmetric combustion chamber, with 720 *mm* length and 133 *mm* inner case diameter, is designated to operate at pressures up to 40 *atm*. Cylindrical one–port high density polyethylene (HDPE) fuel grains, 560 *mm* long, were tested. Four initial inner diameters, 16, 25, 50 and 75 *mm*, were used in order to explore a wide range of mass fluxes, grain length to diameter ratios and injector to grain port diameters ratio. Two chambers were placed before and after the grain; the first one, made by Teflon®, to shift toward the fore end of the grain the strong recirculation region caused by the oxygen injection in an attempt to increase the overall regression rates; the second one, made by stainless steel covered with thermal protections (produced by AVIO), to promote the complete gas mixing, thereby improving the combustion efficiency.

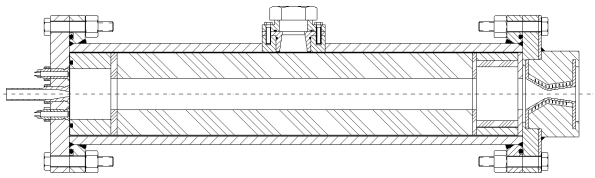

Fig. 1. Hybrid rocket engine scheme

A second series of tests was carried out using a configuration with a radial injector and a dump plenum (in stainless steel); the oxygen injector, shown in Fig. 2, produces a high speed radial flow of oxygen via 16 equally spaced 2.5 *mm* diameter orifices around the periphery of the injector cap. This injection technique should prevent the high recirculation which is yielded by the axial injector instead [1].

In addition, some tests were performed with a metallic grid placed in the dump plenum in order to further eliminate the vortex produced and to provide a relatively uniform flow at the combustion port entry.

A water cooled De Laval nozzle with 16 *mm* throat diameter and 2.44 area ratio, made of copper alloy, ensures long time tests.

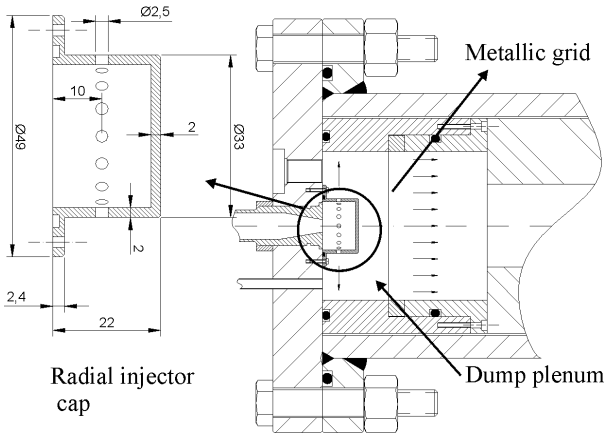

Fig. 2. Radial injector and dump plenum (dimensions are in mm)

Chamber pressure is measured by two capacitive transducers, Setra model 280E, set up in the pre-chamber and in the mixing chamber. All of the signals are sampled at 100 *Hz*, recorded and processed by the software that also controls the system.

The regression rate over time is measured by means of an ultrasounds equipment. One ultrasonic transducer, located around the middle of the chamber (Fig. 1), is employed in order to obtain the time evolution of the local grain thickness and, in turn, the regression rate in that point.

The ultrasonic transducer is a Panametrics Videoscan V114-SB of ¾ *in* nominal diameter and 1 *MHz* central frequency. The signals emitted by the transducer are generated and amplified by a pulser-receiver device (Panametrics

model 5072PR), acquired by an oscilloscope and processed with an oscilloscope proper function which instantaneously computes the time lapse between the trigger event (transmitted wave) and the first zero crossing point with positive slope of the inner surface echo waveform, with 10 *Hz*. This frequency is limited by the oscilloscope performance, anyway, since the fuel may have a regression rate of 1 *mm/s* or lower, for quasi-steady applications it seems a working value. Recently a new technique has been developed for the ultrasound measurements: the ultrasound waveforms are sampled by a National Instruments 5112 PCI digitiser with 100 *MHz* frequency and a repetition frequency equal to 100 *Hz* (ten times higher than the value limited by the oscilloscope). Then the ultrasound signals are analysed by means of a cross correlation technique in order to compute the time delay between two appropriate echoes. This method has been applied only in the tests performed with the radial injector configuration. The grain thickness value was calculated from the waves propagation time considering the wave speed in the fuel to be constant [3]. The thickness data were filtered by applying a Gaussian low-pass filter with a cut-off frequency of 3 *Hz*, then a central formula was applied to take the thickness derivative, i.e. for the regression rate calculation. The time-space-averaged regression rate was simply calculated from the fuel mass loss.

Analysis of results

Time and spatially averaged regression rate is reported in Fig. 3 as a function of the total mass flux together with the data in Refs. [4, 5, 6]. All of the tests in these references were conducted with polyethylene fuel.

According to Fig. 3, at the same mass flux and pressure levels, current regression rates from the axial injection motor differently behaves in terms of both mass flux dependence and magnitude compared to the data in the literature. While it is not proper, in principle, to match up the regression rate magnitude with that of the data from Mitsuno and Lengellé, because of the different oxidiser and its initial temperature, some comparisons can be advanced between the regression rate-mass flux trends. However, present results indicate higher regression rates (up to 2.5 times faster than those in the literature) and lower influence of the mass flux itself as demonstrated by the value of the power law exponent.

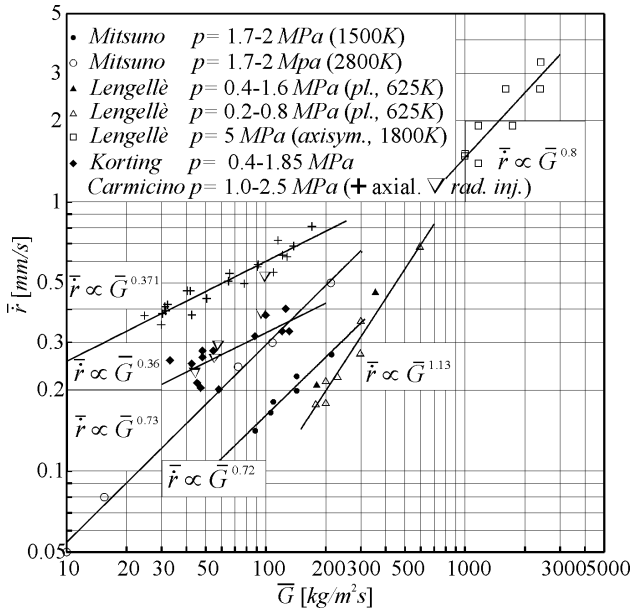

Fig. 3. Comparison of average regression rates

Oxidiser and its entrance temperature apart, the main difference between the experimental conditions in the works of Mitsuno [4], Lengellé [5] and Korting [6] and those in the present one lies in the way the oxidiser is injected into the port. Indeed, in the first three experimental devices there is no nozzle but there is an injector chamber that uniformly distributes the oxidiser at the fuel port inlet. This is the reason of the different regression behaviors. In fact, in our conditions, the oxygen injected by the conical nozzle, generating a flow recirculation zone, leads to a non uniform convective heat transfer distribution in which the wall heat flux and the regression rate increase from a low value just downstream of the prechamber to a maximum at the jet impingement

region, and, further downstream, gradually decrease along the combustor axis.

The examination of the port shape after the test shows fuel consumption profiles consistent with the regression rate distribution described earlier (Fig. 4).

All of the curves in Fig. 4a and Fig. 4b (D_0 = 75, 50 *mm*) display a maximum, whose location, in almost all of the cases, moves downstream as the fuel burns. Different profiles, instead, are exhibited in Fig. 4c and Fig. 4d (D_0 = 25, 16 *mm*) by the curves relative to *Tests* 1, 10, 19 and *Tests* 5 and 18. Fig. 4 also depicts the approximate oxidiser jet diameter, which is plotted by assuming a divergence angle varying between 6° and 8° according to Ref. [7]. The comparison between the jet pattern and the port diameter profiles suggests that the maximum regression rate falls in the region where the oxygen jet impinges on the grain's surface and, therefore, the maximum convective heat transfer is expected. For 25 *mm* and 16 *mm* initial diameter grains this behaviour appears not so marked possibly because of the restricted grain length fraction affected by the jet impingement. Indeed, also in this case, when larger diameters are reached (or higher fuel consumption is realised), i.e. *Test* 6 for D_0 = 25 *mm* and *Test* 3 for D_0 = 16 *mm*, the situation turns quite similar. It is worth noting that this consumption profiles are typical of solid fuel ramjets where a rearward facing step is placed at the air inlet as flame holding. There, combustion occurring in the mixing region preheats oxygen and gaseous fuel available to the leading edge of the diffusion flame increasing the local flame speed beyond the local flow speed so establishing a stable combustion.

As concerns the average regression rates

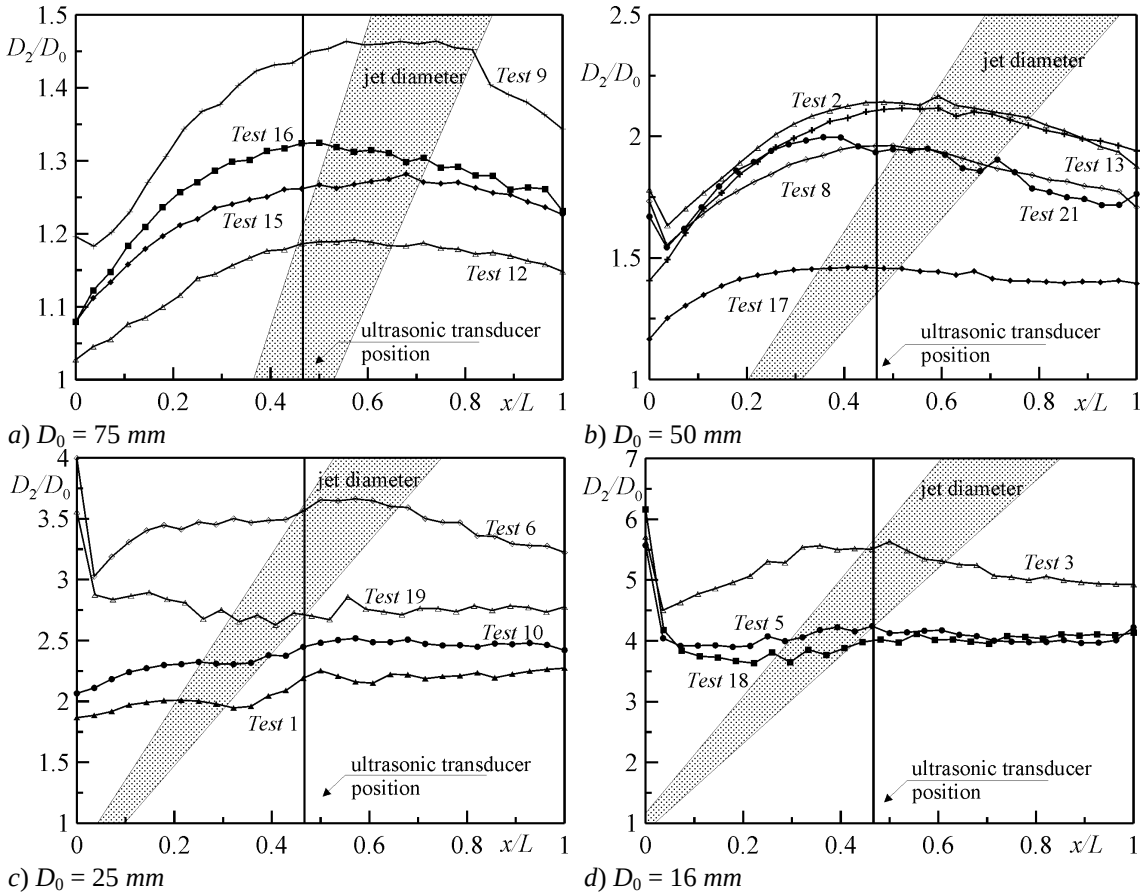

Fig. 4. After burn port diameter profiles (axial injector)

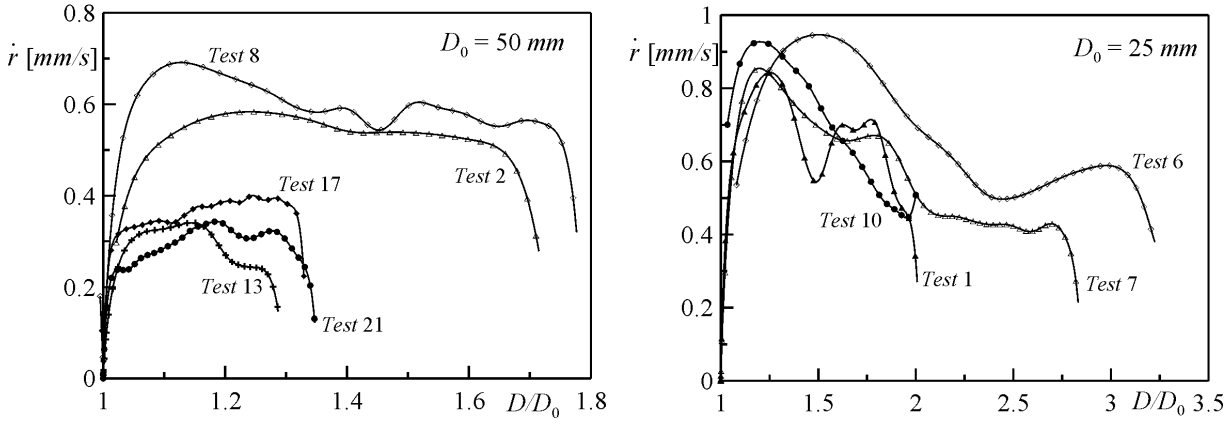

Fig. 5. Local instantaneous regression rates (axial injector)

achieved by means of the radial injection configuration, the latter fall on the experimental data from Korting [6], except the point at the highest mass flux which was affected by wide pressure oscillations as will be discussed later. However, the points at low mass fluxes are too few for inferring a correct trend.

Looking at the instantaneous regression rate curves plotted versus the local instantaneous grain diameter (Fig. 5) can support the existence of a strong injection effect. Qualitatively matching the corresponding data in Fig. 4 and Fig. 5, one sees that, for $D_0 = 50$ *mm*, during the run, the oxygen impacts on the grain at the transducer location and so the local regression rate appears increasing or nearly constant. Substantially different behaviour happens for $D_0 = 25$ *mm*: the regression rate displays a decreasing trend because the region of impingement remains upstream of the transducer except for *Test* 6 in which, actually, the regression rate begins to increase when $D/D_0 \cong 2.4$. *Test* 7 shows similar trend so, although the lack of post-firing port diameter profile, an analogous situation can be supposed. The comparison with the post firing port shape from some tests carried out with the radial injector and the dump plenum allows us to confirm what pointed out earlier. In accordance with the profiles in Fig. 6, for large initial port diameters the fuel consumption distribution is fairly uniform and similar to the ones in Fig. 4c and Fig. 4d ($D_0 = 25$, 16 *mm*) where the port diameter to injector diameter ratio is so small as to reduce the recirculation region extent.

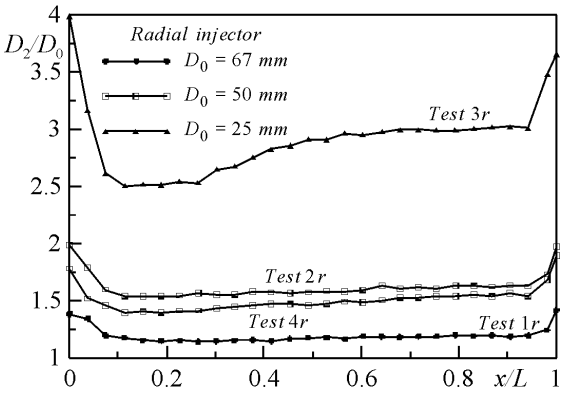

Fig. 6. After burn port diameter profiles (radial injector)

Less uniform consumption is displayed by the port shape of *Test* 3*r* (Fig. 6) where the initial inner diameter is $D_0 = 25$ *mm*. This may be explained by a somewhat strong *vena contracta* effect due to the large sudden contraction the gas undergoes in this case, as it moves from the dump plenum towards the combustion port.With the radial injector the instantaneous regression rate changes as well; indeed, as shown in Fig. 7 where oxidiser mass flux and chamber pressure versus time are reported, the mean trend of regression rate nearly follows the mass flux in contrast to the trends displayed in Fig. 5. Only *Test* 1 and *Test* 10 in this figure

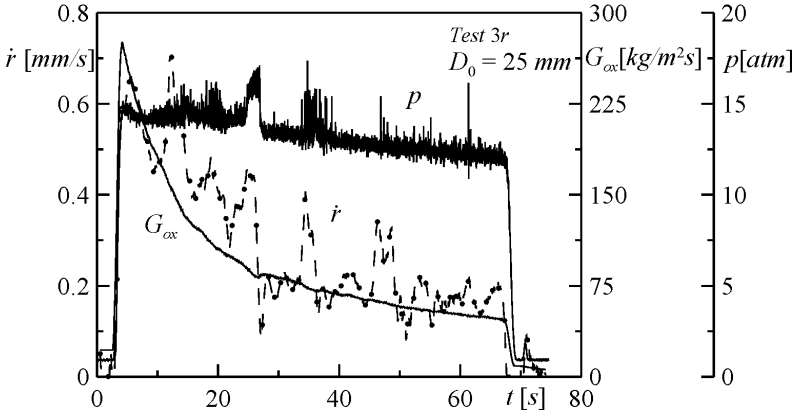

Fig. 7. Local regression rate and oxygen mass flux, chamber pressure (radial injector)

(D_0 = 25 *mm*) can be supposed to have a similar behaviour. For these tests, in fact, the injector effect is almost absent (see Fig. 4c).

Fig. 7 additionally shows the oscillatory behaviour of the chamber pressure which is definitely absent in all of the tests with the axial injector motor. Hence, as expected from the literature [1], the radial injection motor produced unstable combustion characterized by large amplitude pressure oscillations on the order of 5 *atm* which enhanced fuel regression rate as demonstrated by the peaks roughly corresponding to the high pressure oscillations onset. The fact that regression rate increases during pressure oscillation periods has been also documented by Dijkstra [8] and is strikingly evident in the first test performed with the radial injector configuration and the dump plenum followed by the metallic grid. The average regression rate obtained in this test is the highest one represented in Fig. 3, whereas the relative pressure trace is depicted in Fig. 9.

As indicated by the pressure-time plot the oscillations amplitude were amplified as compared to *Test* 3*r* reaching a value around 25 *atm* even higher than the average pressure of 18.5 *atm*. This worse behaviour was expected [1] since the metallic grid lessens the flow recirculation and thus the propellant mixing stabilizing the flame; anyway the pressure oscillation was probably worsened by a coupling be-

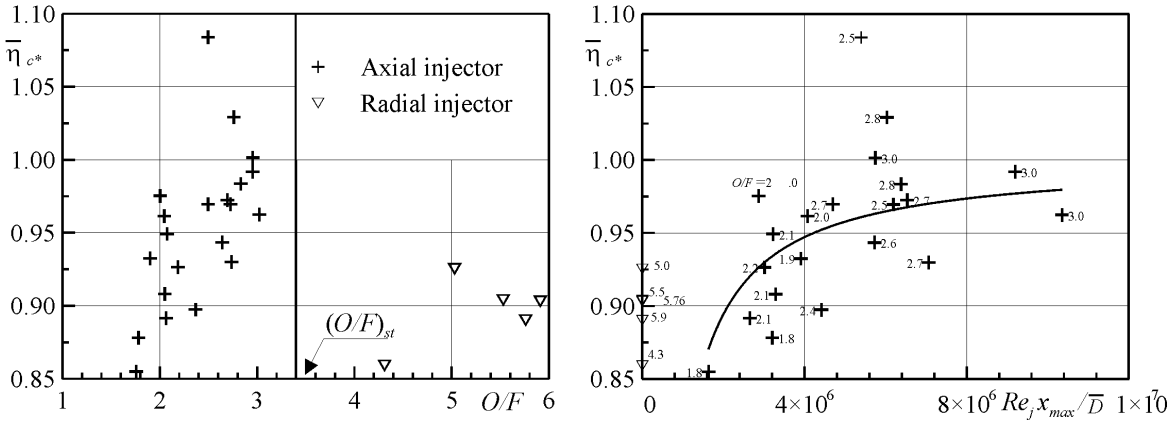

Fig. 8. Combustion efficiency

tween the combustor dynamics and the oxidiser delivery system that is not isolated by any sonic choke. Finally, it is very interesting to look at the combustion efficiency achieved by the axial and the radial injection configurations. Here the efficiency was defined as the ratio between the experimentally measured characteristic exhaust velocity to the theoretical one, the latter computed with the CEA chemical equilibrium code [9].

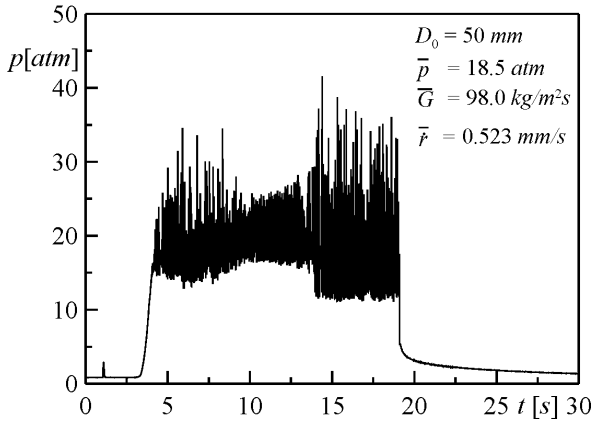

Fig. 9. Chamber pressure (radial injector and metallic grid configuration)

As it is shown in Fig. 8, most of the data from the axial injection motor correspond to efficiency around 95% at fuel rich mixture ratios, while the radial injection motor has lower efficiency with oxidiser rich mixture.This issue is believed to be due again to the recirculation zone present in the axial injection motor that promotes a mixing of oxidiser and fuel in the head-end of the combustor port. This seems confirmed by the second diagram in Fig. 8 where the combustion efficiency was plotted versus the product of the oxidiser jet Reynolds number and the recirculation length to average diameter ratio. This parameter may be qualitatively considered as an index of the mixing strength and its relative extent but, of course, it was introduced just for a rough analysis. In this diagram the points from the radial injection motor were positioned at the origin because the mixing length was considered to be zero. It can be noticed that as the mixing increases the combustion efficiency increases as well.

Conclusions

Injector effects are conceived one of the most important aspects of hybrid combustor design, in fact, they can significantly affect the overall behavior of the motor in terms of such important characteristics as the fuel consumption uniformity, the combustion efficiency and the combustion stability. Since these effects may easily overshadow classical ballistic model calculations, there is a real need to investigate the injector influence in order to develop reliable tools for performance prediction.

This paper dealt with the results of the static engine firings of a hybrid rocket where gaseous oxygen was supplied into axial-symmetric polyethylene cylindrical grains through two different injector configurations: an axial conical subsonic nozzle and a radial injector were tested.

Average regression rates coming from the axial injector motor, exhibited higher values and weaker mass flux dependence. This topic, in conjunction with the higher combustion stability and efficiency renders this configuration particularly attractive. The fuel consumption irregularity, however, has to be better studied in order to reduce the unburned fuel and, at the same time, try to raise the regression rate for motor applications that do not involve the highest thrusts.

References

[1] Boardman, T.A., Brinton D.H., Carpenter, R.L. and Zoladz, T.F. An experimental investigation of pressure oscillations and their suppression in subscale hybrid rocket motors, AIAA paper 95-2689, Jul. 1995.

[2] Russo Sorge, A. The state of art of hybrid propulsion research in Italy, *Proceedings of the 8th International Workshop on Combustion and Propulsion*, Pozzuoli, Jun. 2002, pp. 09-1 – 09-7.

[3] Traineau, J.C. and Kuentzmann, P. Ultrasonic measurements of solid propellant burning rates in nozleless rocket motors, *Journal of Propulsion and Power*, Vol. 2, No. 3, pp. 215-222, 1986.

[4] Mitsuno, M., Kuwabara, T., Kosaka, K., Shirota, K. Experimental study on solid fuel ram rocket, *31st IAF Conference*, Sep. 1980.

[5] Lengellé, G., Fourest, B., Godon, J.C., Guin, C. Condensed phase behavior and ablation rate of fuels for hybrid propulsion, AIAA paper 93-2413, Jun. 1993.

[6] Korting, P.A.O.G., Schöyer, H.F.R and Timnat, Y.M. Advanced hybrid rocket motor experiments, *Acta Astronautica*, Vol. 15, No. 2, pp. 97-104, 1987.

[7] Abramovich, G.N., *The theory of turbulent jets*. Massachussets Institute of Technology, 1963, pp. 3-17.

[8] Dijkstra, F., Korting, P.A.O.G. and van der Berg, R. Ultrasonic regression rate measurement in solid fuel ramjets, AIAA paper 90-1963, Jul. 1990.

[9] Gordon, S., McBride B.J. Computer program of complex chemical equilibrium compositions and applications, NASA Reference Publication 1311, Oct. 1994.